J Solid State Electrochem (2007) 11:155–164
DOI 10.1007/s10008-006-0217-9

ORIGINAL PAPER

Electrochemical deposition of ternary and binary systems from an alkaline electrolyte—a demanding way for manufacturing p-doped bismuth and antimony tellurides for the use in thermoelectric elements

Kerstin Tittes · Waldfried Plieth

Received: 15 March 2006 / Revised: 11 August 2006 / Accepted: 15 August 2006 / Published online: 25 October 2006

Abstract Alkaline solution, especially diphosphate solutions, can be used as electrolytes for the galvanic deposition of p-type semiconductors. A ternary Bi–Sb–Te alloy semiconductor was deposited at a Ni-covered cathode surface at potentials lower than −0.6 V (Ag/AgCl), under potentiostatic condition in well-stirred solutions. Additionally, it was possible to deposit antimony telluride, a binary p-semiconductor, from the ternary electrolyte. The kinetics of the process was investigated by cyclic voltammetric measurements. The influence of the electrolyte convection on the electrocrystallization was analysed with the help of rotating disc electrode. The semiconductor layers were characterized by electrochemical impedance spectroscopy.

Keywords P-semiconductor · Cyclic voltammetry · Electrodeposition · Bismuth–antimony telluride · Antimony telluride

Introduction

Bismuth tellurides are promising materials for thermocouples. They are used in thermoelectrical devices like coolers and thermobatteries. These devices consist of constructive parts, so-called leg materials with high thermoelectric coefficient (α) and a large thermoelectric efficiency ($\alpha/\rho\lambda$), i.e. materials with low thermal conductivity and low electrical resistance (Table 1). P-doped and n-doped bismuth telluride materials can both build up layers with thermoelectric coefficients of |100| to |200| mV/K (296–298 K) [1]; nevertheless, the binary p-type bismuth telluride deposition experiments from acidic electrolytes were not successful [2, 3]. Even the electrodeposition of the ternary system bismuth–antimony–tellurium from acidic and basic electrolytes leads to stable p-conducting structures. The aim of the research was the galvanic deposition of the compound semiconductor with a Bi content of 6–12 at%, 28–34 at% of Sb and a Te amount of 60 at% (Fig. 1). Stecker et al. [4] pointed out that an excess of 2 at% Te would increase the thermoelectric figures of merit of the material. The works of Leimkühler and Kerkamm [5], as well as the publications of Prieto et al. [6], Martin-Gonzales and Prieto [7] and Vereecken et al. [8], were the guidelines for the experiments. Bismuth–antimony tellurides with different contents were deposited from electrolytes, based upon nitric acid developed by Fleurial et al. [3, 9], Martin-Gonzales and Prieto [10] and Snyder et al. [11]. In our work, basic electrolytes [12–15] were used (usually diphosphate) because of the corrosivity of acidic solutions and the lack of solubility of the antimony and tellurium compounds in the nitric acid.

Experimental

The composition of the diphosphate alloy deposition electrolyte, based on a Bi electrolyte, given in Table 2. Potassium diphosphate (>98%; Riedel-de Haen) and diethylene-triamine-pentaacetic acid (DTPA; >99%, Riedel-de Haen) were dissolved in deionized water at 343 K, then bismuth chloride (99.99%; Chempur) was added, and the solution was stirred for 1 h. A solution of potassium–antimony tartrate (99–103%, Riedel-de Haen) was added

Paper presented at the Jahrestagung der Fachgruppe Angewandte Elektrochemie der Gesellschaft Deutscher Chemiker, Düsseldorf, 11.-14.09.2005

K. Tittes (✉) · W. Plieth
Department of Physical Chemistry/Electrochemistry,
Technische Universitaet Dresden,
01062 Dresden, Germany
e-mail: dr.k_tittes@web.de

Table 1 Room temperature values of the Seebeck coefficient (α), Hall mobility (μ), electrical resistivity (ρ), and carrier concentration (n and p) for different semiconductors of Bi and Sb chalcogenides [1]

Films	Bi_2Te_3 n-type	Sb_2Te_3 p-type	$(Bi_{1-x}Sb_x)_2Te_3$; x=0.73; p-type	$(Bi_{1-x}Sb_x)_2Te_3$; x=0.77; p-type	$Bi_2(Se_x)Te_{3-x}$; x=0.3; n-type
α (μV/K)	−213	+110	+240	+21	−200
μ (cm^2/Vs)	52	50	67	76	
ρ (μΩm)	11	4	21	30	
n, p (cm^{-3})	10^{20}	3×10^{20}	5×10^{19}	3×10^{19}	

after cooling. Then the pH value was adjusted at 9, and potassium tellurite hydrate (>95%, Fluka) was added and filtrated subsequently (filter no. 593; Schleicher & Schuell). The composition of the electrolyte varied from 0.05 to 0.14 mol/l Bi, 0.008 to 0.004 mol/l Sb and 0.006 to 0.27 mol/l Te. The concentrations of DTPA and potassium diphosphate were 0.1–0.4 and 0.6 mol/l, respectively.

Copper and nickel foils with a thickness of 50–70 μm were used as substrates for the working electrodes. The foils were degreased by cyclohexane vapour. On the copper samples, 5 μm nickel was deposited from sulphamate electrolyte (pH 4, 313 K). A platinum oxide-doped titanium stretch metal was used as anode. The coated substrate was rinsed after electrolyses with deionized water. Then the samples were dried in air and analysed.

The alloys were deposited under potentiostatic control. Potentials in the range of −0.55 to −0.85 V saturated calomel electrode (SCE) were applied. The electrolyses were carried out in the temperature range of 278–318 K in a stirred solution (magnetic stirrer, 600 rpm). A 263A potentiostat (EG&G) was used for the deposition experiments.

The analyses of the components in the electrolyte occurred by separate processes. The amount of bismuth was determined photometrically with thiourea [16, 17]. The antimony content was titrated bromatometrically [18, 19]. The tellurium concentration was determined potentiometrically by redox titration of the chromium (VI) excess with Fe (II) ions [20, 21].

The ternary electrolyte was investigated by the reverse voltammetric stripping analysis in differential pulse mode [22]. The supporting electrolyte consisted of dilute HCl or $HClO_4$. An indium solution was added to achieve a better separation of the anodic stripping peaks. The measurement was performed at the static mercury drop electrode equipment 303A (EG&G). An EG&G 263A was used as a potentiostat. Two calibration solutions were added for quantitative determinations. The peak currents of bismuth and antimony were used for analyses. The determination of tellurium occurred by cathodic stripping methods after an accumulation step of telluric acid at the mercury drop.

In the case of the use of capillary-active additives in the electrolytes, it was necessary to use inductively coupled plasma optical emission spectroscopy (ICP-OES). The analyses were performed according to DIN EN ISO 11855.

The surface morphology of the deposited alloys was studied by scanning electron microscopy (DSM 982, Zeiss Oberkochen). The bismuth, antimony and tellurium contents of the deposits were investigated with the help of the energy dispersive X-ray microanalyses. An external standard (12 at % Bi, 28 at% Sb, 60 at% Te) was used for these measurements. The concentration of bismuth was determined from the intensities of the M-line; the L-lines were used for antimony and tellurium determination. The acceleration energy was 18 kV. The deposited layers were analysed at five points, and average values of Bi, Sb and Te were calculated. ICP-OES was used for comparable measure-

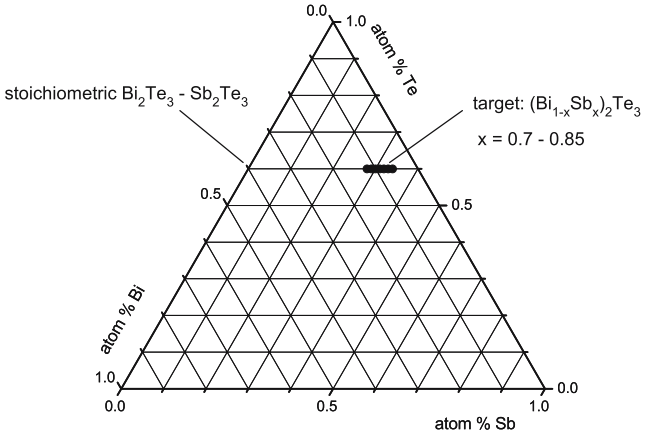

Fig. 1 Ternary phase diagram of the target composition of Bi_2Te_3–Sb_2Te_3 (mole ratio, 1:1)

Table 2 Composition of the diphosphate electrolyte of Bi electrodeposition

Component	Concentration (g/l)
Potassium diphosphate $K_4P_2O_7$	200
Disodium salt of ethylenediamine-tetra acetic acid $C_{10}H_{14}N_2Na_2O_8{\cdot}2H_2O$–EDTA (complexing agent)	150
Bismuth chloride $BiCl_3{\cdot}H_2O$	48
Dextrin (surfactant)	10
Ammonia solution	For adjusting the pH value

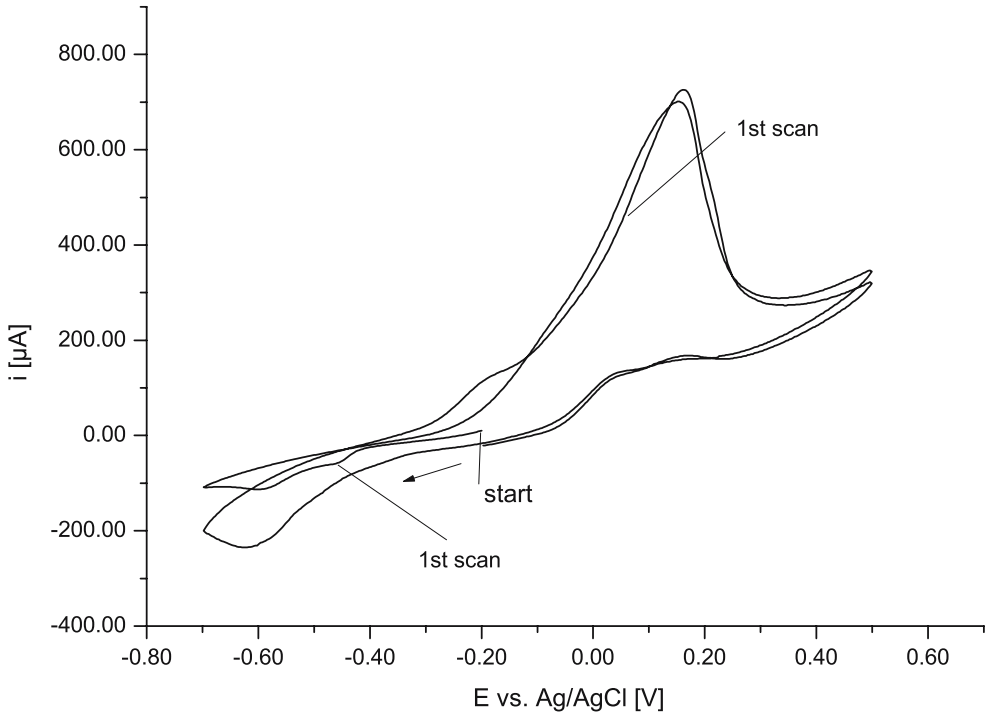

Fig. 2 Cyclic voltammogram of Te deposition on Cu microelectrode—WE: Cu; CE: Pt; RE: Ag/AgCl; 3 mol/l KCl; scan rate 0.05 V/s, supporting electrolyte: 0.6 mol/l $K_4P_2O_7$, pH 9; sample: K_2TeO_3 (0.044 mol/l)–DTPA (0.08 mol/l) electrolyte

ments. The deep profile analyses by glow-discharge OES yielded the quantitative composition of the layers.

The voltammetric investigations were carried out with a 263A potentiostat (EG&G). The reference system was a 3-M Ag/AgCl electrode. A platinum wire was used as a counter electrode in 0.6 M diphosphate solution. The counter and reference electrodes were separated from the sample electrolyte by the so-called Vycor®-tips, microporous glass diffusion barrier pieces. Metal wires (Pt, Cu, Ni), glass sealed and plain polished at the front side with an area of 0.5–0.8 mm^2, acted as working electrodes. Antimony was sealed/moulded in a glass tube and contacted with a copper wire. The pretreatment or regeneration of the working electrodes was done by polishing in combination with rinsing by distilled water. A microcell (EG&G, V=7 ml) was used in most cases for the cyclic voltammetric investigations.

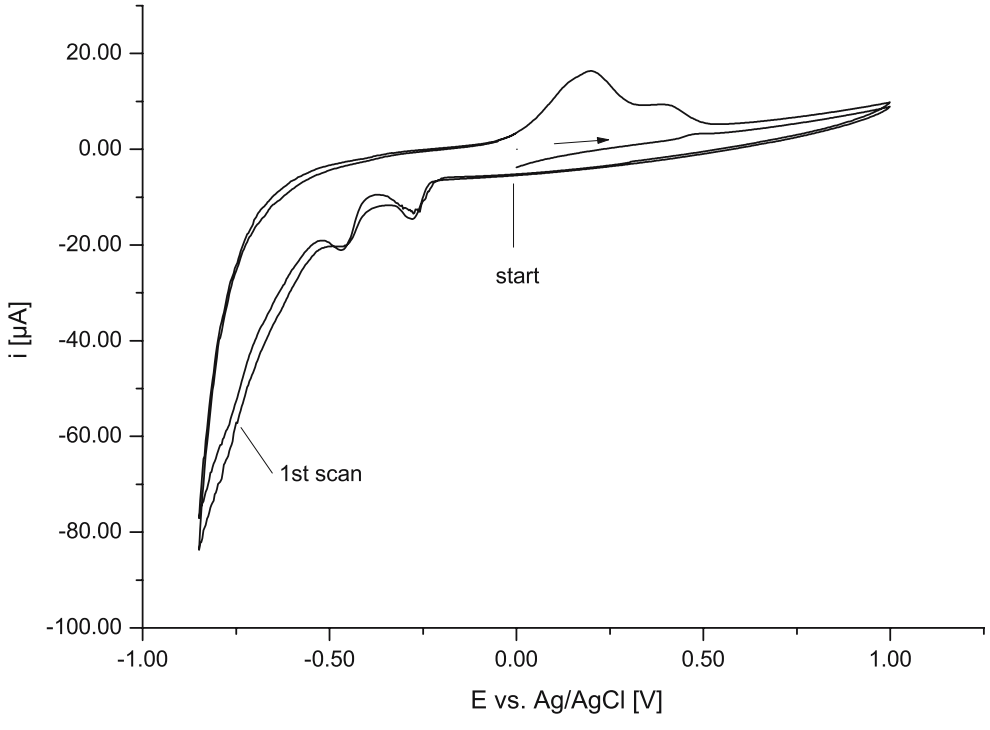

Fig. 3 Cyclic voltammogram of ternary alloy deposition on Ni microelectrode—WE: Ni; CE: Pt; RE: Ag/AgCl; 3 mol/l KCl; scan rate 0.05 V/s, supporting electrolyte: 0.6 mol/l $K_4P_2O_7$, pH 9; sample: ternary (Bi, 12.0×10^{-3} mol/l; Sb, 1.3×10^{-3} mol/l; Te, 2.7×10^{-3} mol/l) electrolyte; DTPA 27.0×10^{-3} mol/l

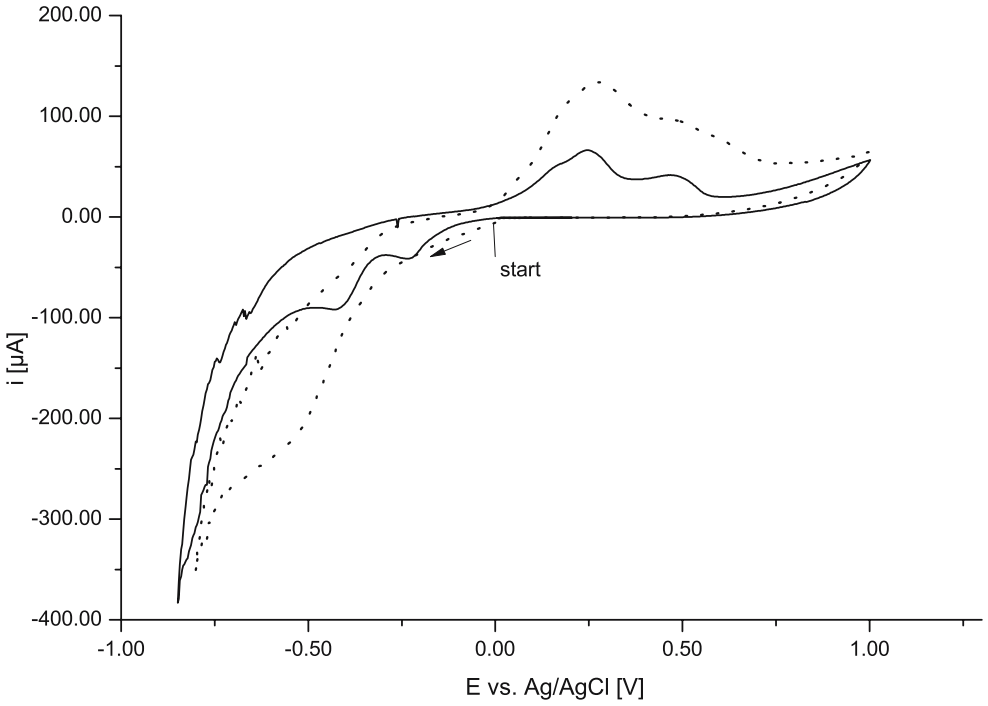

Fig. 4 Cyclic voltammogram of ternary alloy deposition on Ni microelectrode: prior (*full line*) and after (*dashed line*) addition of Bi solution. WE: Ni; CE: Pt; RE: Ag/AgCl; 3 mol/l KCl; scan rate 0.05 V/s, supporting electrolyte: 0.6 mol/l $K_4P_2O_7$, pH 9; sample: ternary (Bi, 12.0×10^{-3} mol/l; Sb, 8.0×10^{-3} mol/l, Te, 2.6×10^{-3} mol/l) electrolyte; DTPA, 26.6×10^{-3} mol/l; Bi concentration after addition: 32.0×10^{-3} mol/l

The influence of convection on the deposition process was studied on rotating platinum disc (A=0.1253 cm^2) working electrode, controlled by a Rotel A-unit (EG&G). The platinum disc was polished with fine alumina down to 0.05-µm grit and carefully rinsed with deionized water prior use. The counter electrode was a Pt disc with an area of 1.41 cm^2. The reference system consisted of a 3-M Ag/AgCl electrode, connected to the cell by a Haber–Luggin capillary, filled with diphosphate electrolyte. As the measuring compartment, a double-walled, thermo-controlled glass cell was used, making experiments possible at different temperatures.

Impedance spectroscopic investigations were carried out in a special cell that could be placed onto the sample surface. The contact area on the sample was 16 mm^2. The measurements were performed under the exclusion of light. A 0.1-M solution of $LiClO_4$ in acetonitrile (p.a. grade, VWR) was used as the supporting electrolyte to prevent chemical

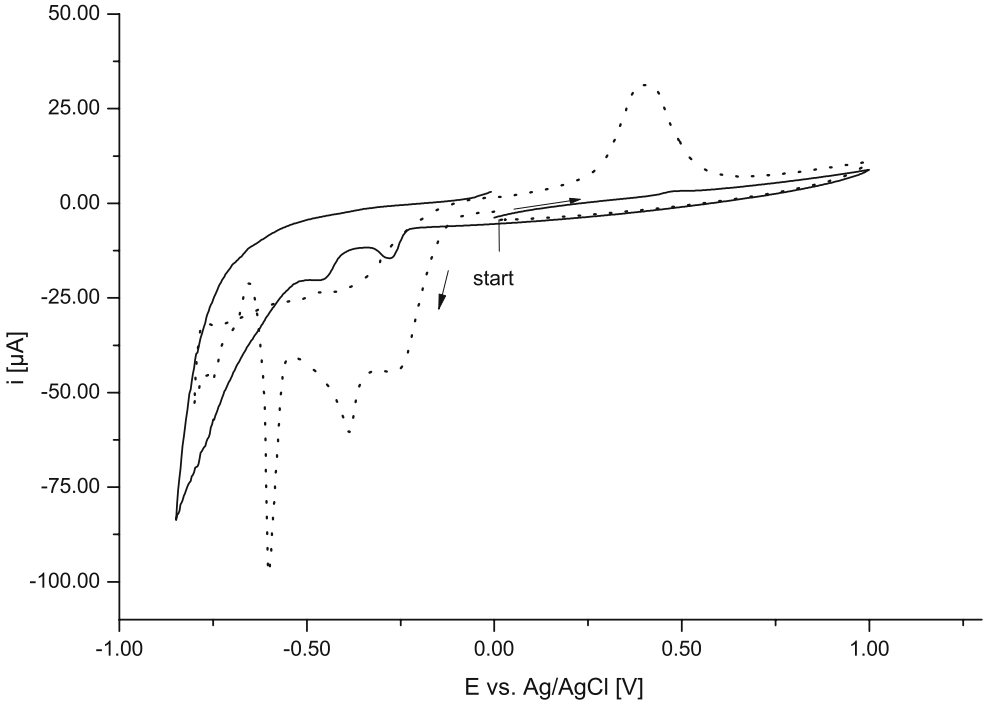

Fig. 5 Cyclic voltammogram of ternary alloy deposition on Ni microelectrode: prior (*full line*) and after (*dashed line*) addition of Te solution. WE: Ni; CE: Pt; RE: Ag/AgCl; 3 mol/l KCl; scan rate 0.05 V/s, supporting electrolyte: 0.6 mol/l $K_4P_2O_7$, pH 9; sample: ternary (Bi, 12.0×10^{-3} mol/l; Sb, 1.3×10^{-3} mol/l; Te, 2.7×10^{-3} mol/l) electrolyte; DTPA, 27.0×10^{-3} mol/l; Te concentration after addition: 93.0×10^{-3} mol/l

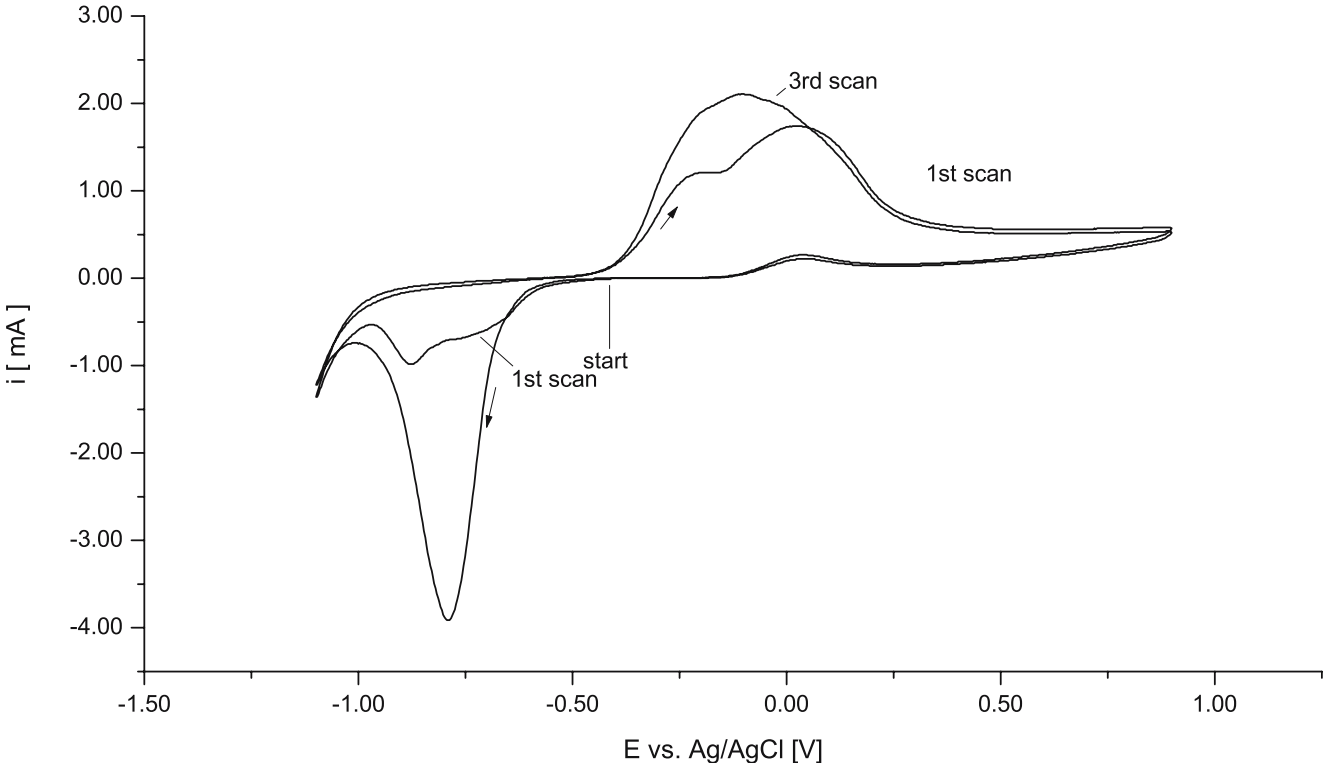

Fig. 6 Formation of ternary alloy layer by anodically dissolved Sb; cyclic voltammogram of Bi–Te electrolyte on Sb microelectrode. WE: Sb; CE: Pt; RE: Ag/AgCl; 3 mol/l KCl; scan rate 0.05 V/s, supporting electrolyte: 0.6 mol/l $K_4P_2O_7$, pH 9; sample: binary (Bi, 0.01 mol/l; Te, 0.014 mol/l) electrolyte

interactions of the semiconductor surface with a protic solvent. The electronic equipment for EIS measurement consisted of a 273A potentiostat (EG&G) coupled with the frequency response analyser SI 1255 (Schlumberger).

Results

The deposition of alloy components on Pt, Cu and Ni microelectrodes was studied by cyclic voltammetry. In the cyclic voltammograms performed at copper electrodes

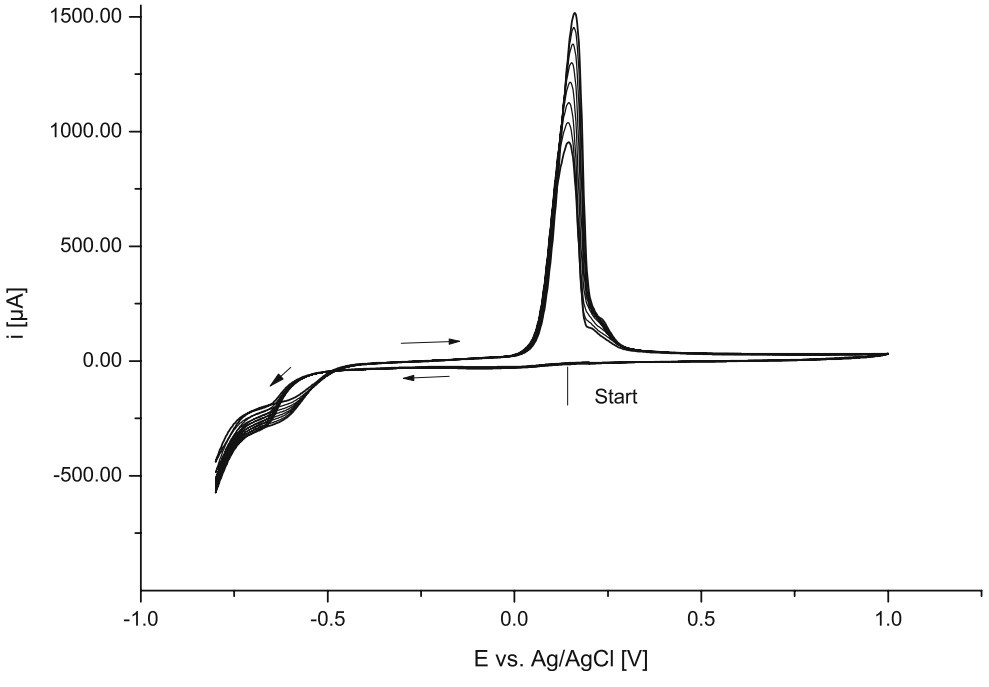

Fig. 7 Ternary alloy deposition dependence on rotation rate. WE: Pt RDE (A=0.126 cm^2); CE: Pt; RE: Ag/AgCl; 3 mol/l KCl; scan rate 0.01 V/s, supporting electrolyte: 0.6 mol/l $K_4P_2O_7$, pH 9; sample: ternary (Bi, 3.0×10^{-3} mol/l; Sb, 0.33×10^{-3} mol/l; Te, 0.33×10^{-3} mol/l; DTPA, 5.3×10^{-3} mol/l) electrolyte rotation velocity: 300, 600, 900, 1,200, 1,500, 1,800, 2,100, 2,400 rpm

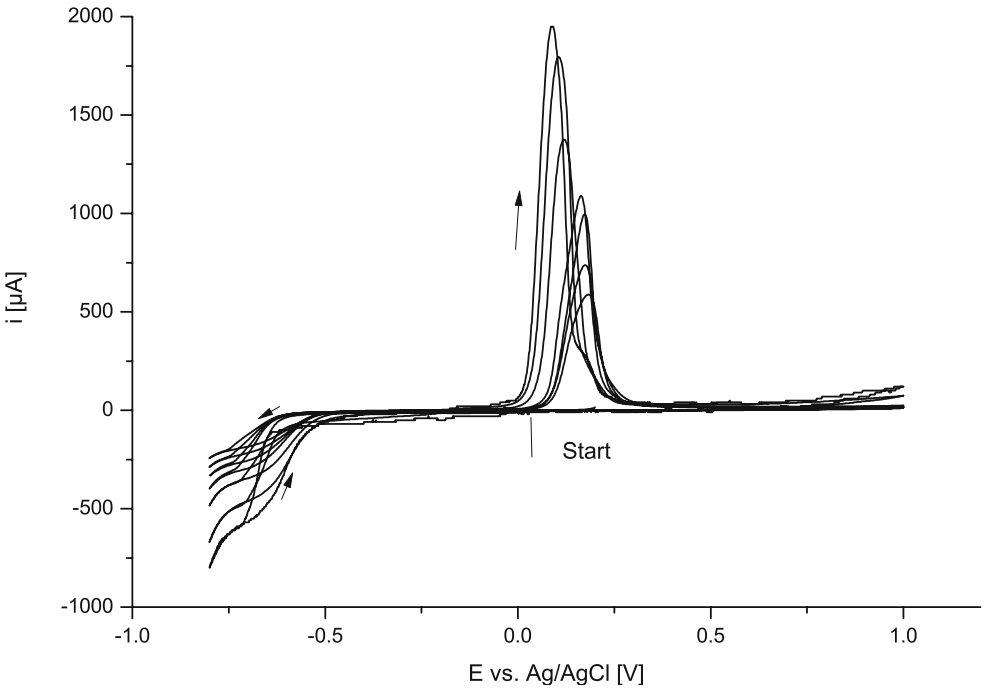

Fig. 8 Ternary alloy deposition dependence on temperature. WE: Pt RDE (A=0.126 cm^2); CE: Pt; RE: Ag/AgCl; 3 mol/l KCl; scan rate 0.01 V/s, supporting electrolyte: 0.6 mol/l $K_4P_2O_7$, pH 9; sample: ternary (Bi, 3.0×10^{-3} mol/l; Sb, 0.33×10^{-3} mol/l; Te, 0.33×10^{-3} mol/l; DTPA, 5.3×10^{-3} mol/l) electrolyte rotation velocity: 1,200 rpm; T: 278, 283, 288, 293, 298, 308, 318 K

(Fig. 2), a relatively small current wave at potentials −0.2 V (SSE) was observed, increasing from cycle to cycle, which was refereed to an accumulation of electrochemically active substances at the advanced potential region. But a much larger asymmetric stripping peak was observed, which could be explained by additional chemical deposition of Te on copper and by the growth of an insoluble layer on the surface; we interpret this as copper telluride layer [23] because this phenomenon was not observed at nickel electrodes concerning of stripping reactions. Both kinetic measurements at microelectrodes as well as galvanic alloy deposition in up-scaled dimensions could be performed at nickel surfaces.

In Fig. 3, it is shown that an alloy deposition was possible from a diphosphate solution on Ni microelectrodes. Peaks appeared at −0.27 V (Ag/AgCl), −0.45 V (Ag/AgCl) and at potentials lower than −0.65 V (SSE), according to the three components of the deposition. If the polarization direction was changed back to positive potentials, a complex anodic stripping peak would be

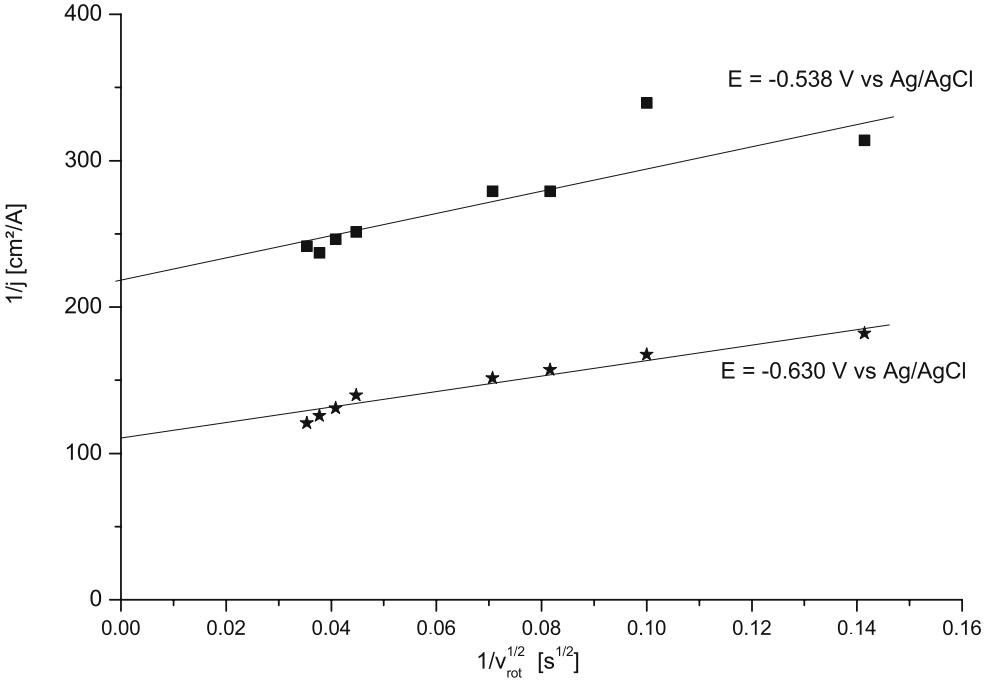

Fig. 9 Investigation of Levich behaviour of the Sb–Te deposition at Pt RDE (A=0.126 cm^2). CE: Pt; RE: Ag/AgCl; 3 mol/l KCl; supporting electrolyte: 0.6 mol/l $K_4P_2O_7$; 3.8×10^{-3} mol/l Sb; 2.3×10^{-3} mol/l Te; 6.4×10^{-2} mol/l DTPA; 293 K

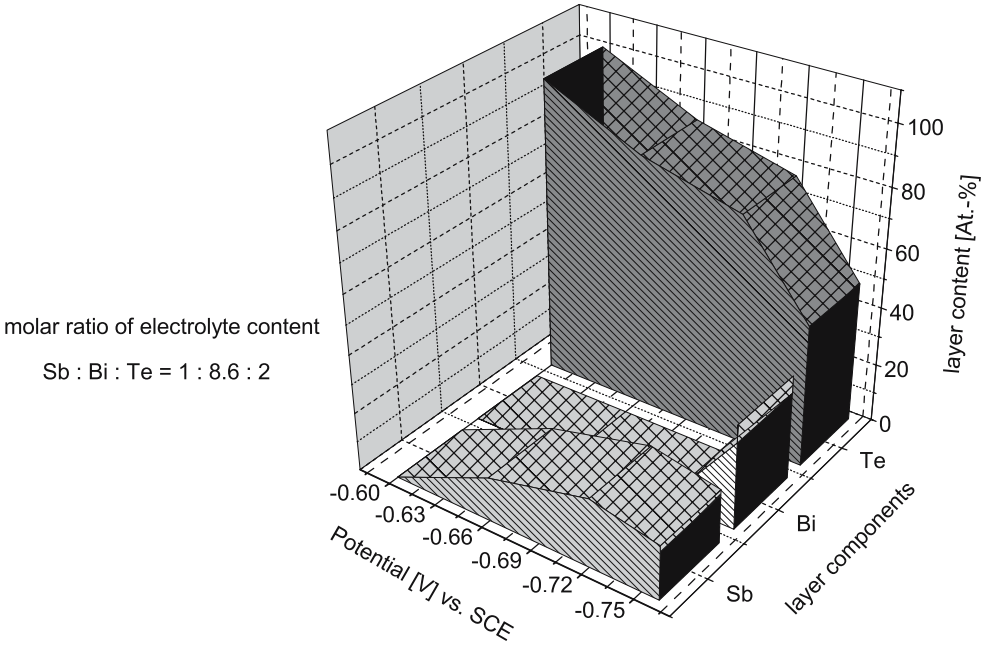

Fig. 10 Dependence of the layer composition on potential mole ratio of the electrolyte: Sb(1)/Bi(8.6)/Te(2)

observed. The identification of the different peaks was possible by sample and hold experiments and by the addition of the different stock solutions of Sb, Te or Bi.

In Fig. 4, if we added a bismuth solution, the characteristic voltammetric behaviour of a bismuth co-deposition can be seen. This process started at potentials at the second cathodic peak. The current increased between −0.5 and −0.75 V (Ag/AgCl). The shape and potential of the corresponding anodic peak showed that an alloy was deposited, not only pure bismuth. An addition of tellurite solution (Fig. 5) led to a broad peak of deposition that was started at −0.27 V (Ag/AgCl). The tellurium deposition influenced the growth of the alloy structure clearly. The stripping peak at 0.4 V (Ag/AgCl) was homogeneous. If an antimony working electrode was used, antimony ions would be released during the anodic treatment. In this case, it was possible to deposit a ternary alloy from the binary Bi–Te electrolyte. The voltammograms in Fig. 6 showed

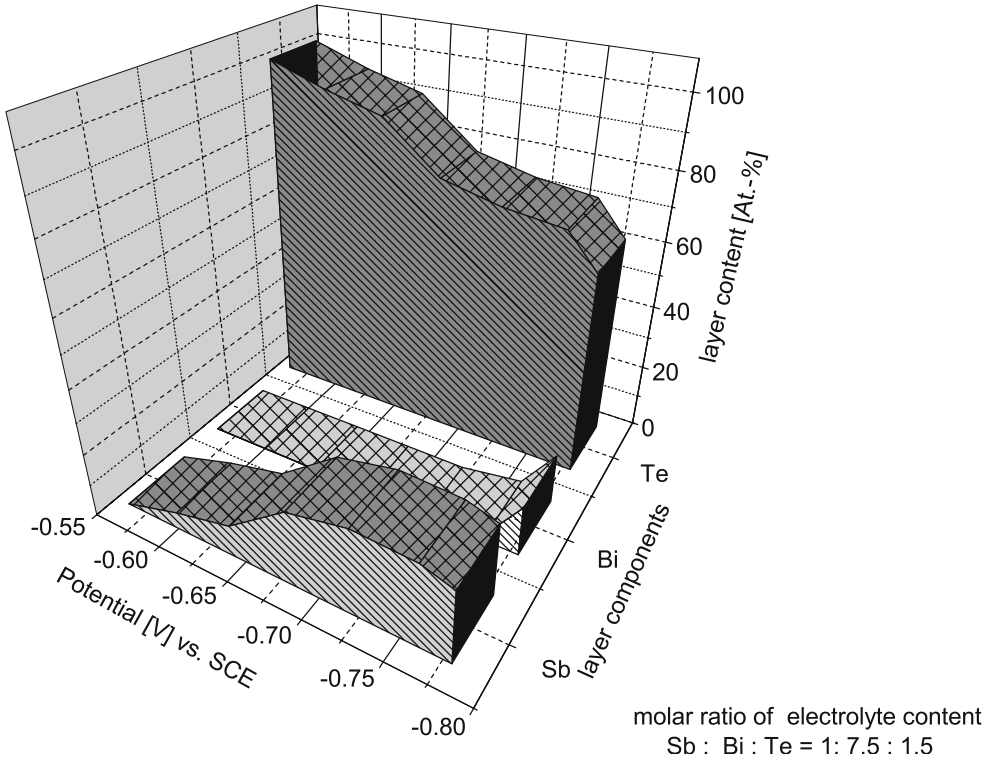

Fig. 11 Dependence of the layer composition on potential mole ratio of the electrolyte: Sb(1)/Bi(7.5)/Te(1.5)

the expected peaks of Te and Te–Bi depositions. The subsequent stripping peaks were a superposition of binary alloy dissolution and antimony oxidizing at 0.0 V (Ag/AgCl). In the cathodic part of the next potential cycle, a new symmetrical peak occurred at −0.76 V (Ag/AgCl), which was interpreted as a ternary alloy deposition, as shown in the following stripping cycle rate.

The dependence of the current potential behaviour on the rotation rate of the platinum disc electrode is shown in Fig. 7. The limiting currents and the peaks of dissolution increased with rotation rates. The stripping peaks showed a symmetrical shape, which indicates a homogenous alloy phase. A shoulder at 0.25 V (Ag/AgCl) could be explained by the dissolution of the primary layer on Pt.

The dependence of the change of the shape of cyclic voltammograms on temperature (Fig. 8) showed that increasing deposition occurred with increasing temperature. The process of electrocrystallization started at slightly positive potentials. The morphology of the alloy deposit was disturbed by higher temperatures; the layers on the disc electrode were rougher, and the layer composition changed. Consequently, electrolyses were performed at a maximum temperature of 293 K for p-type semiconductor deposition. The dependence of current on the velocity of rotation showed Levich behaviour according to Eqs. 1 and 2 [24] in the case of ternary alloy deposition, as well as in the case of binary Sb–Te growth (Fig. 9). The pure activation-controlled current density j_{ac} showed a clear dependence on the applied potential.

$$j_{\lim} = 0.62 n F D^{2/3} \nu^{-1/6} \omega^{1/2} c \tag{1}$$

$$\frac{1}{j} = \frac{1}{j_{ac}} + \frac{1}{B\sqrt{\omega}} \tag{2}$$

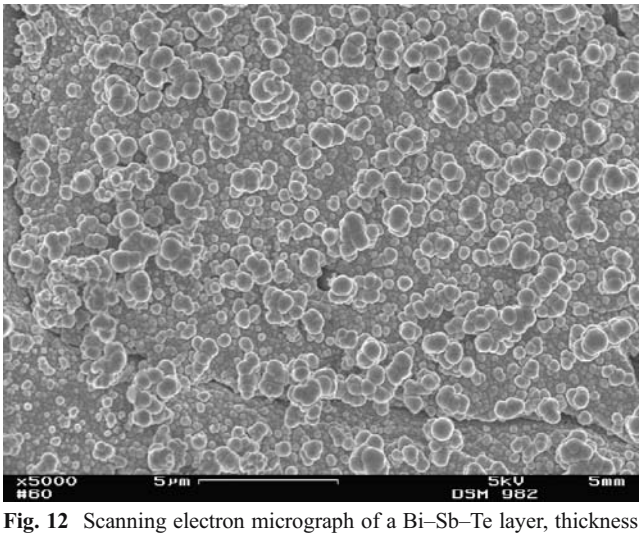

Fig. 12 Scanning electron micrograph of a Bi–Sb–Te layer, thickness 11 µm. X-ray photoelectron spectroscopy analysis: 6 at% Bi; 32 at% Sb; 62 at% Te

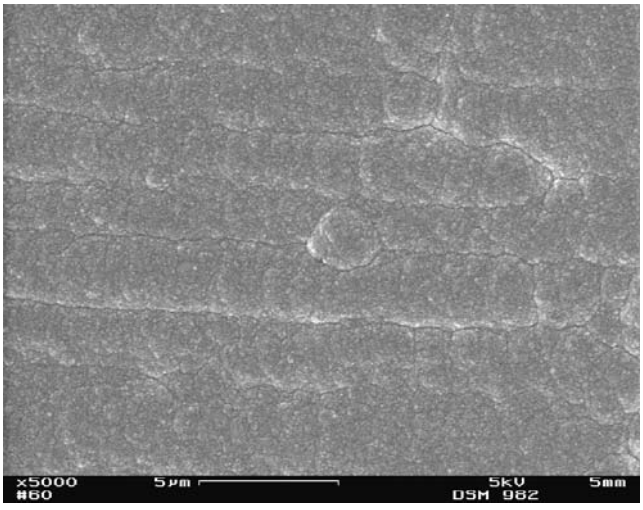

Fig. 13 Scanning electron micrograph of a Sb–Te layer, thickness 12 µm. XPS analysis: 38.4 at% Sb; 61.6 at% Te

where $j_{\lim}$ is the limiting current density, ν is the kinematic viscosity (cm^2/s), ω is the angular velocity ($2\pi\nu_{rot}$, s^{-1}), j_{ac} is the activation controlled current density and B is a constant.

Figures 10 and 11 show the dependence of layer composition on the electrode potential. At lower potential values, the tellurium content in the layer was decreased, and the bismuth content increased. The antimony concentration in the layer showed a maximum of −0.72 V vs. SCE. At higher (negative) potentials and in dependence of electrolyte composition, bismuth and antimony were alloyed.

The micrograph of a bismuth–antimony telluride layer is shown in Fig. 12. The layers were dark grey and rough. The surface became smoother with decreasing bismuth content. Bright metallic galvanic layers, but of binary composition of antimony telluride, were deposited from ternary electrolytes (Fig. 13) at other, more positive potentials. A cross

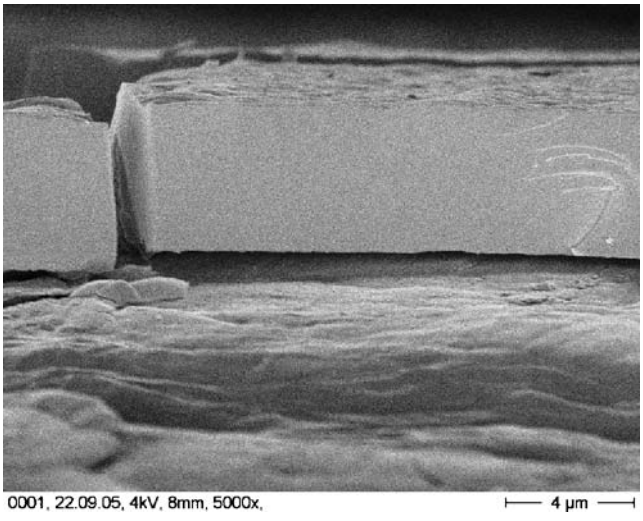

Fig. 14 Scanning electron micrograph of a Sb–Te layer, cross section prepared by tensile fracture

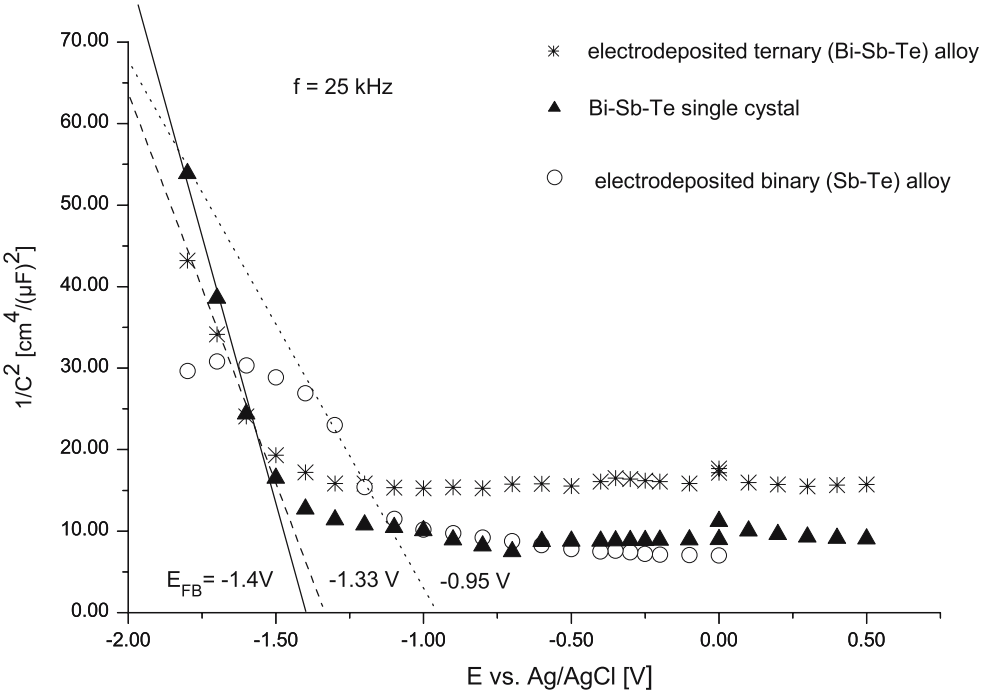

Fig. 15 Investigation of semiconductor characteristic: Mott–Schottky plot. Electrodeposited Bi–Sb–Te alloy (*asterisk*): carrier density, $N^+=1.5\times10^{17}$–$1.9\times10^{17}/cm^3$; $E_{fb}=-1.33$ V (Ag/AgCl); layer composition: 6 at% Bi, 32 at% Sb, 62 at% Te. Electrodeposited Sb–Te alloy (*circle*): carrier density, $N^+=2.1\times10^{17}$–$2.7\times10^{17}/cm^3$; $E_{fb}=-0.95$ V (Ag/AgCl); layer composition: 38.4 at% Sb, 61.6 at% Te. Bi–Sb–Te single crystal, synthesized after the Bridgman method (*filled triangle*): carrier density, $N^+=1.1\times10^{17}$–$1.3\times10^{17}/cm^3$; $E_{fb}=-1.4$ V (Ag/AgCl); crystal composition: 12 at% Bi, 28 at% Sb, 60 at% Te

section of a binary alloy, deposited from Sb–Te electrolyte, embrittled by liquid nitrogen and prepared by tensile fracture technique, showed the same smooth surface and a fine layer structure (Fig. 14).

To characterize the semiconductor properties of the deposited layers, the EIS was used. The dependence of the space charge capacity of the semiconductor on the applied potentials, as $1/C^2$ versus E plots (Mott–Schottky) [25], gave the flatband potential from the intercept of the plot with the *x*-axis. The sign of the slope showed the type of the semiconductor (p, n). The charge carrier concentration could be calculated from the slope. In Fig. 15, the Mott–Schottky plots of different samples are shown at a frequency of 25 kHz. The negative sign of the slope of a deposited Bi–Sb–Te layer gave the p-type character of the sample. The flatband potential E_{fb} would yield −1.33 V, the carrier concentration 1.5×10^{17}–$1.9\times10^{17}/cm^3$, if we assume a dielectric constant ε_r of 8–10 [26]. The measured concentration was 2 orders of magnitude lower than values in the literature (Table 1). The Mott–Schottky plot of antimony telluride, also p-type, gave a carrier concentration of 2.1×10^{17}–$2.7\times10^{17}/cm^3$ higher than in ternary alloys. A reference Bi–Sb–Te crystal, made by the so-called Bridgman technique, was investigated under the same conditions with the identically measuring cell with nearly the same experimental results.

Figure 16 shows an example of telluride electrodeposition on commercially used wafer structures. The deposition in wafer trenches demonstrated the possibility of electrochemical semiconductor microdeposition.

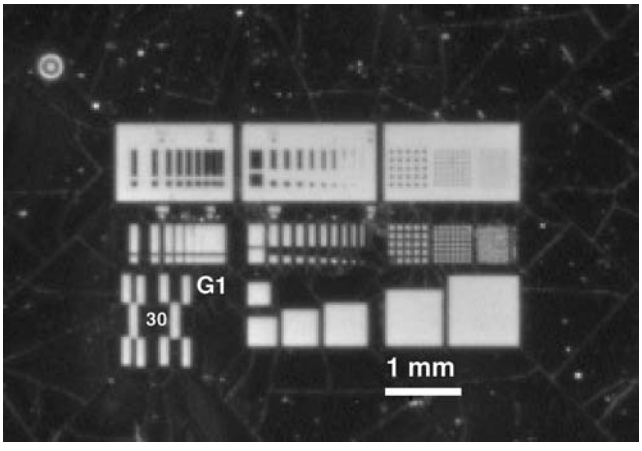

Fig. 16 Light optical micrograph of a 4-in. wafer, electrochemically coated with antimony telluride from diphosphate electrolyte

Conclusions

The electrochemical deposition of p-type semiconducting bismuth–antimony tellurides or antimony tellurides from diphosphate electrolytes was demonstrated. Nickel or nickel-covered surfaces are the suitable substrates for the telluride deposition. In the case of a ternary alloy, it is necessary to work under potentiostatic control. The process temperature should not exceed 293 K. A controlled agitation of the electrolyte is of striking importance for a semiconductor layer of a good quality. The charge carrier concentration of the electrodeposited ternary alloy was smaller by a factor of 100 compared with the current literature.

Acknowledgements This study was supported by the BMWi (Bundesministerium für Wirtschaft) and the AiF (Arbeitsgemeinschaft industrieller Forschungsvereinigungen "Otto von Guericke" e. V.) research no. 13936 BR. The authors are grateful to Dr. M. Stölzer (Physical Department of the Martin Luther University, Halle, Germany) for the preparation of the Bi–Sb–Te reference samples and Dr. C. Blank (Institute of Material Science of the Technical University Dresden, Germany) for carrying out of optical microscopy and the excellent Sb_2Te_3 layer on substrate preparation for SEM. The wafer material was supplied by Semiconductor Technology and Microsystems Laboratory, Technical University Dresden.

References

1. Boulouz A, Charkrabarty S, Giani A (2001) J Appl Phys 89:5009
2. Tittes K, Plieth W, Plötner M, Qu W, Fischer WJ (2001) Mikrogalvanische Abscheidung thermoelektrisch aktiver Verbindungen für die Anwendung als Spannungsversorgung in autarken Mikrosystemen Abschlussbericht AiF-Projekt Nr. 12118BR, TU Dresden
3. Fleurial JP, Herman AJ, Snyder GJ, Ryan MA, Borshchevsky A, Huang CK (2000) Mater Res Soc Symp Proc 626:Z11.3.1
4. Stecker A, Stordeur M, Langhammer HT (1986) In: Unger K, Schneider HG (eds) Verbindungshalbleiter. Akademische Verlagsgesellschaft Geest & Portig KG, Leipzig, p 333
5. Leimkühler G, Kerkamm I (2002) J Electrochem Soc 149(10): C474
6. Prieto AL, Martin-Gonzales M, Keyani (2003) J Am Chem Soc 125:2388
7. Martin-Gonzales M, Prieto AL (2003) Chem Mater 15:1676
8. Vereecken PM, Ren S, Sun L, Searson PL (2003) J Electrochem Soc 150(3):C131
9. Fleurial JP, Borshchevsky A, Ryan MA (1999) Mater Res Soc Symp Proc 545:493
10. Martin-Gonzales M, Prieto AL (2003) Adv Mater 5(12):1003
11. Snyder GJ, Lim J, Huang CK, Fleurial JP (2003) Nat Mat 2:528
12. Kotschman ED, Gamer PU (1978) Zashita Metallov 16:493
13. Anonym (1982) Met Finish 80:31
14. Campell F, Fraunhofer JA (1976) Surf Technol 4:303
15. McCarthy JA (1963) Met Finish 61:58
16. Mahr C (1933) Z Analyt Chemie 94:161
17. Mahr C (1934) Z Analyt Chemie 97:96
18. Schulze G, Herrmann J (1989) Jander–Jahr Maßanalyse 15. Auflage Walter de Gryter, Berlin, p 181
19. Autorenkollektiv (1974) Lehrwerk Chemie-Arbeitsbuch 5 Elektrolytgleichgewichte und Elektrochemie, VEB Deutscher Verlag für Grundstoffindustrie, Leipzig, p 111
20. Lenher V, Wakefield HF (1923) J Am Chem Soc 45:1423
21. Lang R, Faude E (1937) Z Analyt Chemie 108:260
22. Haase HJ (1996) Elektrochemische stripping-analyse, VCH Verlagsgesellschaft mbH, Weinheim
23. Maclachlan JB, Kruesi WH, Fray DJ (1992) J Mater Sci 27 (15):4223
24. Gileadi E (1993) Electrode kinetics for chemists, chemical engineers, and material scientists. VCH Inc., New York
25. Vijakumar A, Du T, Sundaram KB (2005) Appl Surf Sci 242:168
26. Black MR, Lin YM, Cronin SB, Rabin O, Dresselhaus MS (2001) Studies of the dielectric constant of thin film Bi nanowire samples using optical reflectometry in anisotropic nanoparticles: synthesis, characterization and applications. In: Stranik S et al (eds) MRS symposium proceedings, Boston, Dec. 2000, Mat Res Soc Press, Pittsburgh, Pennsylvania